

Design and structure–activity relationship of 3-benzimidazol-2-yl-1*H*-indazoles as inhibitors of receptor tyrosine kinases

Christopher M. McBride, Paul A. Renhowe, Carla Heise, Johanna M. Jansen, Gena Lapointe, Sylvia Ma, Ramon Piñeda, Jayesh Vora, Marion Wiesmann and Cynthia M. Shafer*

Small Molecule Drug Discovery, Biopharma Division, Chiron Corporation, 4560 Horton Street, Emeryville, CA 94608, USA

Received 22 February 2006; revised 20 March 2006; accepted 21 March 2006

Available online 5 April 2006

Abstract—3-Benzimidazol-2-yl-1*H*-indazole analogs were developed as inhibitors of receptor tyrosine kinases (RTK). The synthesis and SAR of this series is reported.

© 2006 Elsevier Ltd. All rights reserved.

Tumor angiogenesis is the process that leads to the formation of blood vessels in a tumor, which in turn supports cancer cell survival, local tumor growth, and the development of distant metastasis.^{1–3} The key mediator of this process is vascular endothelial growth factor (VEGF) binding to its respective receptor tyrosine kinase (RTK) to promote the proliferation, migration, and survival of endothelial cells. Additional pro-angiogenic RTKs and their growth factors are basic fibroblast growth factor (bFGF) and platelet derived growth factor (PDGF) with additional functions in early angiogenesis and the stabilization of newly formed blood vessels, respectively. Demonstration of several tumors to secrete VEGF has made VEGFR-2 as well as PDGFR and FGFR expression aid tumorigenesis directly with autocrine and/or paracrine signaling through these receptors, resulting in deregulated autonomous growth.^{4,5} Therefore blocking, in particular, VEGF signaling through these receptors has become an attractive target for anti-cancer therapy. The approaches to block signaling include the neutralizing anti-VEGF antibody, soluble VEGF receptors, antisense oligonucleotides targeting VEGF, and small molecule inhibitors of the receptor tyrosine kinases. There are multiple RTK inhibitors in development targeting VEGFR-2 and in some cases

PDGFR. The most advanced small molecule inhibitors, BAY43-9006 and SU11248, have both been approved for advanced renal cell carcinoma,^{6,7} while PTK787 is currently in Phase III trials.⁸

During the course of our RTK inhibitor program, we desired an alternate scaffold to the 4-amino-3-benzimidazol-2-ylhydroquinolin-2-one series (Fig. 1, **1**).^{9–12} One idea entailed contracting the B ring from a 6-membered ring to a 5-membered ring which would change the orientation of the benzimidazole (rings C and D) relative to the B ring, while retaining the donor–acceptor–donor motif necessary for binding to the hinge region of the RTKs. The scaffold that arose from this effort was the 3-benzimidazol-2-yl-1*H*-indazole scaffold (**2**, hereafter referred to as indazole benzimidazole). While the unadorned indazole benzimidazole (**2**) exhibited

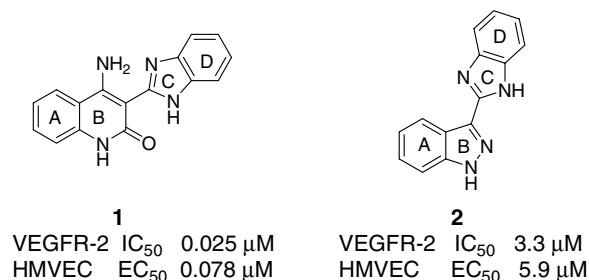


Figure 1. Potency of 4-Amino-3-benzimidazol-2-ylhydroquinolin-2-one (**1**) and 3-Benzimidazol-2-yl-1*H*-indazole (**2**) in VEGFR-2 and inhibition of VEGF-mediated proliferation of endothelial cells (HMVEC).

Keywords: Indazole benzimidazole; Receptor tyrosine kinase (RTK); Vascular endothelial growth factor (VEGF); Basic fibroblast growth factor (bFGF); Platelet derived growth factor (PDGF).

*Corresponding author. Tel.: +1 510 923 8086; e-mail: cynthia_shafer@chiron.com

significantly less activity against VEGFR-2 compared to the unsubstituted 4-amino-3-benzimidazol-2-ylhydroquinolin-2-one (**1**), we felt this series could be optimized to yield potent RTK inhibitors. A dedicated effort ensued to improve the affinity of this scaffold toward VEGFR-2 and the other RTKs of interest and to explore the SAR of this series.¹³

Initially, a number of basic amines were surveyed on the D ring to attempt to improve both in vitro potency and solubility. Substitution of the 4' position of the benzimidazole with morpholine (**Table 1**, **3**) led to loss of activity, while moving the morpholine to the 5' position (**4**) improved affinity 20-fold over the unsubstituted indazole benzimidazole (**2**). Replacing the morpholine with 1-methylpiperazine (**5**) yielded similar affinity but somewhat improved the inhibition of VEGF-mediated proliferation of endothelial cells (HMVEC). The piperidinylpiperidine substituent (**6**) conferred even greater potency against VEGFR-2, while retaining the good cellular activity achieved with 1-methylpiperazine. Substitution with an acyclic amine (**7**) showed similar potency to the cyclic amines **4** and **5**. In addition to basic amines, a number of other substituents were tolerated

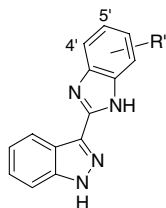
on ring D, including aromatic heterocycles (**8**), ethers (**9**) and alkylamino heterocycles (**10**).

Because of the attractive in vitro profile of **6**, the SAR of the A ring was investigated using the 5'-piperidinylpiperidine D ring substituent. Substitution at C-4 of ring A was sensitive to the nature of the substituent (**Table 2**, **11–12**) with the 4-benzyloxy substituent resulting in lower VEGFR-2 affinity, while the 4-*tert*-butyl urea gave equipotent affinity compared to **6**.

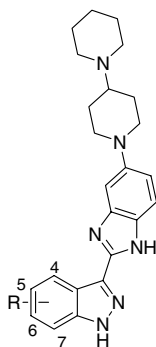
A diverse group of substituents were incorporated at C-5 and C-6, and found to have improved enzymatic potencies (**Table 2**, **13–20**) compared to unsubstituted **6**. Potency in cells, however, was static or worse, except when electronegative substituents, such as fluoro (**18**) and trifluoromethyl (**20**), were incorporated at C-6, which presumably increased the lipophilicity of the molecules and thus improved permeability of the compounds through the cell membrane. At C-7, fluorine (**21**) was the only substituent that maintained activity.

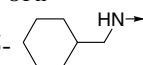
Our program focused on VEGFR-2 affinity but considered concurrent affinity for VEGFR-1, PDGFR β , and

Table 1. Structure–activity relationship of substituents on ring D of the indazole benzimidazole



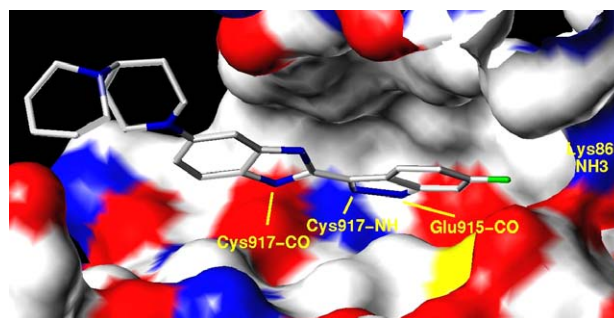
Compound	R'	VEGFR-2 ¹⁴ IC ₅₀ (μM)	VEGFR-1 IC ₅₀ (μM)	PDGFR β ¹⁴ IC ₅₀ (μM)	FGFR-1 IC ₅₀ (μM)	HMVEC EC ₅₀ (μM)
2	H	3.3	0.72	3.4	1.4	5.9
3	4'-	>3.0	>3.0	>3.0	0.83	>10
4	5'-	0.16	0.050	0.26	0.10	0.16
5	5'-	0.13	0.044	0.17	0.082	0.097
6	5'-	0.078	0.028	0.69	0.048	0.097
7	5'-	0.15	0.008	0.50	0.018	0.22
8	5'-	0.083	0.096	1.4	0.21	7.0
9	5'-	0.17	0.048	0.44	0.098	0.27
10	5'-	0.26	0.17	1.9	0.27	0.30

Table 2. Structure–activity relationship of substituents on ring A of the indazole benzimidazole

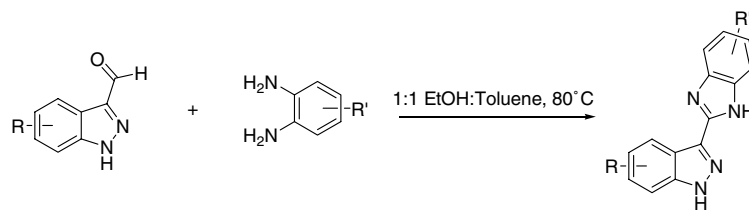
Compound	R	VEGFR-2 IC ₅₀ (μM)	VEGFR-1 IC ₅₀ (μM)	PDGFRβ IC ₅₀ (μM)	FGFR-1 IC ₅₀ (μM)	HMVEC EC ₅₀ (μM)
6	H	0.078	0.028	0.69	0.048	0.097
11	4-OBn	0.66	0.063	1.8	0.094	0.46
12	4-NH(CO)NH <i>t</i> -Bu	0.070	0.004	0.44	0.003	0.24
13	5-OBn	0.030	0.003	0.083	0.008	0.19
14	5-OPh	0.044	0.028	0.008	0.015	0.080
15	5- 	0.044	0.021	1.7	0.016	0.22
16	5-NH(CO)NH <i>t</i> -Bu	0.005	0.001	0.081	0.001	0.35
17	5-CO ₂ Me	0.031	0.015	0.063	0.073	0.13
18	6-F	0.028	0.010	0.31	0.028	0.033
19	6-OBn	0.021	0.011	0.18	0.023	0.22
20	6-CF ₃	0.052	0.002	0.062	0.002	0.004
21	7-F	0.33	0.15	2.3	0.20	1.4
22	7-OBn	>3.0	>3.0	>3.0	>3.0	1.8
23	7-NH(CO)NH <i>t</i> -Bu	>3.0	>3.0	>3.0	>3.0	—

FGFR-1 to be advantageous. For the indazole benzimidazole series, VEGFR-1 and FGFR-1 affinity tracked consistently for most compounds and was typically better than VEGFR-2 affinity. While the compounds did exhibit affinity for PDGFRβ, they were typically 2- to 39-fold less potent against PDGFRβ than VEGFR-2. Compound **14**, however, showed 5-fold selectivity for PDGFRβ over VEGFR-2 suggesting the 5-phenoxy as a potential starting point for PDGFRβ selective compounds. Conversely, the aliphatic 5-cyclohexylmethyl amine substituent (**15**) yielded significantly lower affinity against PDGFRβ while retaining potency against the other RTKs. These observations of various kinase selectivity profiles make this series an interesting tool to begin examining the effect of such profiles on cell-based activity and efficacy.

In order to rationalize the observed SAR from a 3D structural perspective, a homology model for VEGFR-2 was built and used to dock representative ligands.¹⁵ Figure 2 shows the docking model for compound **18**, with three hydrogen bonds from the indazole benzimidazole core to the hinge domain and the 5'-piperidinylpiperidine substituent pointing out into solvent. This model suggests that one tautomer for the benzimidazole substructure will be preferred in order to present a hydrogen bond donor to the hinge domain. Substitution on the C-4 position with a hydrogen bond donor as in compound **12** will drive the tautomeric equilibrium to the desired form, while substitution with a hydrogen

**Figure 2.** Docking model of compound **18** in VEGFR-2 homology model. Surface of the binding site is colored by atom-type (Oxygen, red; Nitrogen, blue; and Carbon, white). Hydrogen bonds to hinge residues are labeled, as is the surface from the catalytic Lys866.

bond acceptor (**13**) will drive the equilibrium to the undesired form. The SAR confirms this hypothesis. The model further supports the observation that substitutions in the 5- and 6-positions are well tolerated. The 6-position gives access to the well-known selectivity pocket, which in Figure 2 is located behind Lys866. The high affinity of 5-substituted compound **16** can be rationalized by the observation that the *tert*-butylurea will be oriented similar to the same substituent in Pfizer's FGFR1 inhibitor, PD173074,^{16,17} which was the ligand in the FGFR1 crystal structure used as the template for the homology modeling. The additional affinity is most likely due to the hydrophobic interac-



Scheme 1. Synthetic scheme for indazole benzimidazoles.

tions of the *tert*-butyl group with the P-loop. The model finally confirms that substituents on the 7-position of the A-ring and the 4'-position of the D-ring are not tolerated due to collisions with the protein.

The observations above deal with the general features of a proposed VEGFR-2 binding site. The kinase inhibition data for this series show varying selectivity profiles. Since the RTKs investigated in this paper are very homologous, the differences in SAR must be governed by subtle differences in the respective active sites of these kinases.

The indazole benzimidazole core is easily assembled from an indazole aldehyde and a phenylenediamine (Scheme 1) in modest yields (30–50%). While some indazole aldehydes are commercially available, most were synthesized from the corresponding indoles¹⁸ via a nitrosation-rearrangement in modest to good yields (50–80%).^{19–22} Additional analogs (e.g., **13**, **15–16**, and **23**) could be synthesized following construction of the core indazole benzimidazole by carrying a nitro through the reaction sequence from commercially available 4-, 5- or 7-nitroindole. Subsequent catalytic reduction followed by reaction with electrophiles gave the desired products.

The pharmacokinetic properties of **18** were examined, and it showed an oral bioavailability of 62%, a $t_{1/2}$ of 253 min, a clearance of 71 mL/min/kg, a volume of distribution of 24.8 L/kg, and an AUC of 170 mg min/mL. This compound was further evaluated in angiogenesis and tumor xenograft models. All doses tested completely inhibited neovascularization in the murine matrigel

model (Fig. 3). Administration of 30 or 100 mpk qd of compound **18** for 14 days resulted in 50% and 88% tumor growth inhibition in the KM12L4a colon tumor model in nude mice and was well tolerated.

In conclusion, a versatile scaffold was developed which had potent inhibitory effects against the receptor tyrosine kinases involved in angiogenesis and blood vessel maintenance. In addition, compound **18** was shown to have favorable pharmacokinetics and exhibit impressive tumor growth inhibition.

Acknowledgments

The authors acknowledge William McCrea for the synthesis of the nitroaniline used to synthesize compound **10**, Timothy Machajewski and Brandon Doughan for providing elemental analysis data for compound **18**, and Helen Ye for performing the matrigel and tumor xenograft experiments.

Supplementary data

Supplementary data associated with this article can be found, in the online version, at [doi:10.1016/j.bmcl.2006.03.069](https://doi.org/10.1016/j.bmcl.2006.03.069).

References and notes

- Folkman, J. *Nat. Med.* **1995**, *1*, 27.
- Kerbel, R. S. *Carcinogenesis* **2000**, *21*, 505.
- Carmeliet, P. *Nat. Med.* **2003**, *9*, 653.
- Ferrara, N. *Oncologist* **2004**, *9*, 2.
- Blume-Jensen, P.; Hunter, T. *Nature* **2001**, *411*, 355.
- 'FDA Approves New Treatment for Advanced Kidney Cancer,' The Food and Drug Administration Press Release, 2005.
- 'FDA Approves Pfizer's Sutent for Kidney and Bowel Cancers,' Pfizer, Inc., 2006.
- Hecht, J. R.; Trarbach, T.; Jaeger, E.; Hainsworth, J.; Wolff, R.; Lloyd, K.; Bodoky, G.; Borner, M.; Laurent, D.; Jacques, C. In *41st ASCO Annual Meeting*; Orlando, FL, 2005; Vol. 3.
- Antonios-McCrea, W. R.; Frazier, K. A.; Jazan, E. M.; Machajewski, T. D.; McBride, C. M.; Pecchi, S.; Renhowe, P. A.; Shafer, C. M.; Taylor, C. *Tetrahedron Lett.* **2006**, *47*, 657.
- Lopes de Menezes, D. E.; Peng, J.; Garrett, E. N.; Louie, S. G.; Lee, S. H.; Wiesmann, M.; Tang, Y.; Shephard, L.; Goldbeck, C.; Oei, Y.; Ye, H.; Aukerman, S. L.; Heise, C. *Clin. Cancer Res.* **2005**, *11*, 5281.

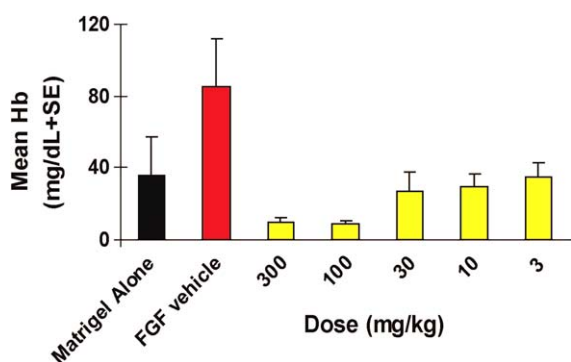


Figure 3. Mice were implanted with FGF supplemented matrigel and administered compound **18** daily for 7 days. Hemoglobin concentrations were determined in the excised matrigel plugs.

11. Shafer, C. M. *Abstracts of Papers*, 228th ACS National Meeting, Philadelphia, PA, United States, August 22–26, 2004; 2004; ORGN-248.
12. The lead compound from this series, CHIR-258, is currently in Phase I clinical trials.
13. During the course of this project, two patent applications on indazole benzimidazole compounds as tyrosine kinase and serine–threonine kinase inhibitors were published (WO 2001002369 and WO 2001053268). The compounds described in those publications, however, were significantly different so as to not affect our program.
14. For both of the biochemical VEGFR2 and PDGFR β assays, the highly conserved mouse homologues have been used.
15. The VEGFR-2 homology model was built using Chemical Computing Group's MOE software. Default settings were used in the alignment and homology modeling module and the FGFR1 crystal structure (2FGI) from the Brookhaven Protein Data Bank was used as a template. Compound **18** was built and optimized in the active site of the homology model using the Flo+apr2003 software from ThistleSoft.
16. Supplemental materials contains an overlay of compound **16** and PD173074.
17. Mohammadi, M.; Froum, S.; Hamby, J. M.; Schroeder, M. C.; Panek, R. L.; Lu, G. H.; Eliseenkova, A. V.; Green, D.; Schlessinger, J.; Hubbard, S. R. *EMBO J.* **1998**, *17*, 5896.
18. Anderson, W. K.; Gopalsamy, A.; Reddy, P. S. *J. Med. Chem.* **1994**, *37*, 1955.
19. Buchi, G.; Lee, G. C. M.; Yang, D.; Tannenbaum, S. R. *J. Am. Chem. Soc.* **1986**, *108*, 4115.
20. Allen, D. G.; Eldred, C. D.; Judkins, B. D.; Mitchell, W. L. In *PCT Int. Appl.*: WO 9749699, 1997; pp. 40.
21. 6-Fluoroindazole aldehyde (3.25 g, 19.8 mmol, 1.0 eq) and 4-(4-piperidylpiperidyl)benzene-1,2-diamine (5.41 g, 19.7 mmol, 1.0 eq) were dissolved in toluene and EtOH (5:1), and heated at 70 °C under N₂. After 2 h, the reaction was opened to the atmosphere, and air was bubbled into the reaction mixture using a fritted gas inlet tube for 20 min. After heating overnight at 70 °C, the reaction mixture was concentrated to give a brown solid which was purified by reverse phase HPLC. The TFA salt was freebased by dissolving in EtOAc and washing the organic layer with NaHCO₃ (aq, satd), water, and brine. The organic layer was then dried over Na₂SO₄, filtered, and concentrated. The HCl salt was added by taking up the free base in 1:1 CH₃CN:H₂O and adding HCl (2 M) until the solid dissolved. The solution was lyophilized to give **18** as a yellow solid (2.1 g, 63%).
22. Further synthetic details and characterization for **18** are included in the Supplemental Material.